Proceedings of the ASME 2014 Pressure Vessels & Piping Conference
PVP2014
July 20-24, 2014, Anaheim, California, USA

PVP2014-28138

STRESS ANALYSIS OF BULGES IN CYLINDRICAL AND OVAL PRESSURE VESSELS

Mahmod Samman
Houston Engineering Solutions
15915 Katy Freeway
Suite 150
Houston, TX 77094, USA
+1(832)512-0109
mms@hes.us.com

Mohammad Samman
Cockrell School of Engineering
University of Texas at Austin
Austin, TX, USA

ABSTRACT

The stress field in and around bulges in cylindrical and oval pressure vessels is examined using linear elastic finite element models. The effects of bulge size and shape on axial and hoop stresses are examined under internal pressure loading. Stress components at the center of the bulge, in the entire bulge, and in the vessel outside the bulge are analyzed both on the inside and outside surfaces of the vessel wall. In addition, the effects of vessel ovality (out-of-roundness) and the location of a bulge relative to ovality on these stress components are studied. This study provides engineers with a detailed look at bulging-induced stresses and the limitations of stress-based fitness-for-service assessment of bulges in pressure vessels such as refinery coke drums.

NOMENCLATURE

σ	stress component
p	pressure
r	vessel radius
t	wall thickness

INTRODUCTION

Under internal pressure, the wall of a long cylindrical vessel with a large diameter-to-thickness ratio experiences a mostly biaxial stress field. Nominal axial and hoop stresses are:

$$\sigma_{axial} = \frac{pr}{2t} \quad (1)$$

$$\sigma_{hoop} = \frac{pr}{t} \quad (2)$$

This nominal stress field changes when a geometric imperfection such as a localized bulge or ovality (out-of-roundness) is present. Higher localized stresses and strains can potentially lead to global failure (plastic collapse), local failure, buckling, or fatigue failures.

The impact of geometric imperfections on the mechanical integrity of pressure vessels is a major concern for engineers in process industries such as refineries and petrochemical plants. The API 579-1/ ASME FFS-1 Standard of 2007 is a widely-used document that provides methods for the fitness-for-service assessment of pressurized equipment with various types of defects. Part 8 of the Standard addresses weld misalignment and shell distortions including bulges and out-of-roundness. The Standard provides three assessment levels that vary in conservatism, limitations, and complexity. Level 1 is the most

conservative and simplest. Level 3 is the most complex and has the least limitations.

According to the Standard, Level 1 assessment of bulges is conducted based on fabrication tolerances of the original construction code. Level 3 assessment of bulges is a comprehensive analysis that requires the use of numerical techniques such as the finite element method. Absent from the document is the Level 2 assessment procedure that was included in the first edition of the document of 2000 when it was an API Recommended Practice. The old assessment method was removed because of potentially misleading and un-conservative results that users may obtain from the stress-based assessment method. Since then, several unsuccessful attempts have been made to develop alternate closed-form stress-based solutions. At the time of writing this paper, no Level 2 assessment technique is expected to be included in the upcoming 2014 edition of the Standard.

Bulges are different from other vessel defects in two ways:

(1) The creation of a bulge typically involves high strains and complex patterns of residual stresses that are difficult to predict and simulate, and
(2) Just like architectural arches and domes, bulges in cylindrical shells can increase local stiffness and enable them to better resist certain types of loads. This effect may be misinterpreted as a benefit to having bulges in pressure vessels.

Typically, bulges in internally-pressurized vessels can result in two failure modes: local failure and/ or fatigue. The common assumption that failures in cyclically loaded equipment at discontinuities are solely due to fatigue is not necessarily accurate.

Coke drums which are large cylindrical refinery vessels usually experience bulging under their normal operating conditions. Typically, the severe cyclic thermo-mechanical loads that develop in these vessels result in multiple large and sometimes interconnected bulges that can increase the diameter of the vessel by several inches. Bulging is usually combined with significant global and/or local ovality. These vessels, which probably represent the most extreme case of bulging in industry, commonly experience cracking at the peak of bulges and less frequently at their trough. Due to the complex and random nature of the thermo-mechanical loads that they experience, a full Level 3 assessment per Annex B1 of API 579-1/ASME FFS-1 is infeasible.

Linear elastic stress analysis of bulged drums under unit internal pressure loading has been attempted in an effort to determine the severity of bulging and predict the likelihood of bulging failures in coke drums. Our experience suggests that neither the magnitude nor location of maximum stress amplification at bulges correlate well with reported failures. In addition, our experience suggests that cracks induced by bulging alone are likely initiated by excessive strain (local failure) and not fatigue.

Because of the above difficulties with stress analysis of bulges, there is a need to better understand stress fields in and around bulges especially when combined with ovality. This study examines the effects of bulges and ovality on the stress field in cylindrical vessels using finite element models. The study is limited to linear elastic stress analysis under internal pressure and excludes the effects of residual stresses and strains that may be present in and around bulges. As with all such numerical simulations, findings of this study may not be applicable to all geometries and loads.

MODEL

The general-purpose finite element analysis software Abaqus was used to create and solve the models of this report.

The study was based on the following:

- Vessel dimensions:
  - 120” radius
  - 500” tangent-to-tangent length
  - 2:1 ellipsoidal top head
  - 60” long support skirt
  - 45° conical bottom head
  - 1” wall thickness
- Material: Steel with a linear elastic model
  - Elastic Modulus = 30E6 psi
  - Poisson’s Ratio = .3
- Linear-geometry solution

Shell models were created using three-dimensional linear quadrilateral reduced-integration shell elements. Models were loaded (except for the support skirt) with a uniform pressure of 10 psi and were restrained in all three directions of translation at the bottom edge of the skirt.

Stress fields in the vessel were examined due to:

a. bulging,
b. vessel ovality, and
c. both.

The models used in this study were built using the following vessel geometry and loading:

p = 10 psi,
r = 120”, and
t = 1”.

Under these conditions, Equations 1 and 2 can be used to calculate nominal axial and hoop stresses of 600 psi and 1200 psi, respectively.

As shown in Figure 2, “Bulge depth” is defined as the maximum distance of bulge protrusion from the body of the vessel. For example, the peak of a two-inch deep bulge is two inches outside the vessel wall. A fillet radius defines the concave transition between bulge and vessel. As fillet radius increases, the transition area becomes longer. The aspect ratio of a bulge is defined as the length (circumferential distance) of the bulge divided by its width (axial distance). These lengths are straight distances calculated between the far edges of transition fillets.

The surface of a bulge is modeled as a sphere, an ellipsoid, or an axisymmetric geometry (uniform profile around circumference). Except for the axisymmetric geometry, bulges

are defined using a "vertical radius" and a "horizontal radius". In a sphere, the radii are equal and, hence, curvature is the same in both directions. In an ellipsoid, they are unequal and curvature is not the same. An axisymmetric bulge is defined only using a vertical radius. Bulges were simulated at mid-height of the vessel.

In the case of spherical bulges, aspect ratio is directly proportional to the radius of the sphere. In ellipsoidal bulges, it is a function of the two radii of the ellipse. For axisymmetric bulges, since an aspect ratio is not definable, the representative large number of 10 is used.

For oval vessels, the ovality ratio is defined as the ratio of the length of the major axis to that of the minor axis of the vessel. The ratios 1.25, 1.54, and 2.00 are considered in this study. While a ratio of 2.0 is unusually large for global vessel ovalization, such a ratio is commonly encountered in localized ovality of vessels with large diameter-to-thickness ratios such as coke drums.

A total of twenty three models were utilized in this study, as shown in tables 1 and 2. An example mesh is shown in Figure 1. In six of the models, both ovality and bulging were present. Since stress fields are influenced by the location of a bulge relative to an oval cylinder, bulges were simulated both on the "short side" and the "long side" of oval vessels as shown in Figure 2.

RESULTS

Examples contour plots of the four stress components (axial inside, axial outside, hoop inside, and hoop outside) are shown in an axisymmetric bulge in Figures 3 to 6, in a vessel with an axisymmetric bulge in Figures 7 to 10, in a local bulge in Figures 11 to 14, and in a vessel with a local bulge in Figures 15 to 18.

Using these models, we studied the relationship between the following parameters and the stress field:

- Fillet Radius
- Bulge Depth
- Bulge aspect ratio
- Vessel ovality ratio

Results are summarized using graphs that relate stress concentration factors (SCF) to above parameters. The SCF is found by dividing axial or circumferential stresses by the respective nominal stress of the undistorted vessel:

From each model, SCFs were reported per location, magnitude, and type as follows:

- Location on vessel:
  - *Center of bulge* refers to the farthest point from the axis of the vessel in the bulge.
  - *Bulge* refers to the convex part of the bulge only (i.e. exclusive of the fillet).
  - *Vessel* refers to the entire model excluding the "bulge", both heads, and skirt.
- Extreme values: maximum and minimum values within a specified region.
- Stress component: axial and circumferential (hoop).
- Surface of the wall: inside and outside.

DISCUSSION

Some of the key observations are discussed below. In the discussion below, unless stated otherwise, SCFs refer to maximum values at stated locations.

Round vessel

- Effect of bulge depth:
  - *Center of bulge*: Hoop and axial SCFs had very different trends, Figure 19. Hoop SCFs were always in tension, less than nominal (under 1.0), and mostly unchanged versus depth. At the minimum depth, axial SCF was 1.2 (tension) and -0.1 (compression) on the inside and outside surfaces, respectively. At maximum depth, axial SCFs on the inside and outside surfaces switched magnitude and direction (tension to compression and vice versa).
  - *Bulge*: All four SCF components were in tension, higher than 1.0, and increased with the increase of bulge depth, Figure 20. SCF components increased more on the outside surface than they did on the inside. On both surfaces, axial SCFs were comparable but slightly higher than hoop SCFs.
  - *Vessel*: Maximum SCF components were in tension, higher than 1.0, and increased with the increase of bulge depth, Figure 21. Minimum SCF components which were in tension but lower than 1.0 at the smallest bulge decreased with the increase of depth until they became compressive at the deepest bulge (with the exception of hoop SCF on the outside surface which remained in tension).
- Effect of fillet radius
  - *Center of bulge*: Hoop and axial SCFs stayed mostly unchanged versus fillet radius, Figure 22. It is important to note that, for the bulges in this graph, all hoop and axial SCFs at the center of the bulge were significantly less than 1.0.
  - *Bulge*: Maximum hoop and axial SCFs decreased in the bulge by approximately 10% as fillet radius increased from 20 to 80 inches, Figure 22. For a bulge depth of 2 inches and vertical and horizontal radii of 100 inches, maximum hoop and axial SCFs in the bulge were all between 1.4 and 2.5. Outside surface SCFs were higher than those on the inside surface.
  - *Vessel*: Maximum hoop and axial SCFs were comparable in magnitude to those in the bulge, Figure 23. Minimum hoop and axial SCFs on the outside and inside surfaces were tensile and mostly compressive, respectively. For a bulge depth of 2 inches and vertical and horizontal radii of 100 inches, all hoop and axial SCFs in the vessel were between -0.5 and 2.8. Maximum SCFs on the outside surface were higher than those on the inside surface.
- Effect of aspect ratio:
  - In the graphs below, the aspect ratio of 10 represents axisymmetric bulges.

- *Center of bulge*: Bulges in Figure 24 have a depth of 2" and a fillet radius of 40". At low aspect ratios, axial SCFs at the center of the bulge on the inside and outside surfaces are similar and less than unity. They both start in compression and become in tension with the increase of aspect ratio. At the extreme high end of aspect ratio, when the bulge becomes axisymmetric, the SCFs diverge, increase in magnitude (more than unity), and become opposite in sign (inside in compression and outside in tension). This suggests that axial bending is relatively small at the center of this localized spherical bulge, but becomes dominant as length increases relative to width. The opposite is true for hoop bending which is significant at low aspect ratios with the inside in tension and outside in compression. As aspect ratio increases, hoop SCF on the inside and outside decrease in magnitude until they intersect and then change sides. At the extreme, when the bulge turns axisymmetric, the inside becomes in compression and outside in tension. The patterns described above are only true for the bulge depth of 2". As shown in Figure 25, SCF magnitudes and trends significantly vary when the depth of the bulge increases from 2" to 4".
- *Bulge*: Maximum SCFs in entire bulges exhibit totally different patterns from those at the center of bulges. Figure 26 and 27 show trends for the same bulges in Figures 24 and 25, respectively. By examining these graphs, two conclusions can be made: (1) maximum SCFs in bulges are not located at the center of bulges, and (2) SCFs in bulges do not follow a clear trend in relation to bulge's aspect ratios.
- *Vessel*: Figure 28 shows an example of the variation of maximum and minimum SCFs in the vessel as a function of a bulge's aspect ratio. The non-monotonic curves demonstrate that, similar to SCFs in bulges, no clear trend can be established between the stress field and a bulge's aspect ratio. Also, compared to Figure 24, it is clear that a bulge may result in SCFs in the vessel that are significantly higher than SCFs in the bulge itself.

Oval vessel

An oval vessel under pressure develops SCFs proportional to the degree of ovality. However, as shown in Figure 29, axial SCFs are significantly larger than hoop SCFs both on the inside and outside surfaces of the wall. At the high end of the range, when ovality ratio is 2, axial SCFs approach 15 on the tension side and 25 on the compression side. At the low end of 1.25, axial SCFs are at 5.

When a 2" bulge is located on the short side of the oval vessel, SCFs in the vessel (outside the bulge) change in different manners, Figure 30. Compared to the same oval vessel without the bulge, compressive axial SCFs increase but tensile axial SCFs decrease. As for the hoop direction, both tensile and compressive SCFs increase. However, when the bulge is located on the long side of the oval, almost the opposite happens, Figure 31. Compressive axial SCFs decrease but tensile axial SCFs increase. In the hoop direction, tensile and compressive SCFs are little changed.

As shown in Figures 32 and 33, to a large extent, the same patterns described above for SCFs in the vessel apply to those in the respective bulges. Magnitudes of SCFs are slightly lower in bulges than they are in vessels.

The most profound effect of bulge location relative to vessel ovality is one observed at the center of the bulge. As shown in Figure 34, SCFs at the center of the bulge reverse direction (tension to compression) and can be several times larger in magnitude depending on where the bulge is located relative to drum ovality. In most cases, the effect of ovality on SCFs is more significant than that of bulging.

CONCLUSION

This limited scope study clearly explains the difficulty that has been encountered in fitness-for-service assessment of bulges using stress analysis techniques. Some of the key findings are:

- Stresses at the center of a bulge can be significantly lower than nominal stresses in the vessel without a bulge. In most cases examined, if stresses at the center of a bulge were to be used for fitness-for-service assessment, the user would come up with the erroneous conclusion that the vessel would be better off with the presence of a bulge.
- Maximum stresses are often located in the vessel outside the bulge.
- Maximum stresses in the bulge and vessel are directly and almost linearly proportional to the depth of the bulge.
- The fillet radius of the transition between bulge and vessel has a relatively minor effect on stresses in the bulge and vessel.
- Stresses in the bulge and vessel can be highly influenced by and have a non-monotonic relationship with the bulge's aspect ratio.
- Vessel ovality and the location of a bulge relative to an oval vessel can have more impact on stresses in the bulge and vessel than bulging does.

This study explains why the assessment of bulges in pressure vessels using linear elastic stress analysis may lead to erroneous conclusions especially when the dominant failure mode is strain-based and when a bulge is located in a vessel with global and/or local ovality.

REFERENCES

(1) API 579-1/ ASME FFS-1 Standard for Fitness-For-Service (2007) American Society of Mechanical Engineers, New York.
(2) Recommended Practice 579 for Fitness-For-Service (2000) American Petroleum Institute, Washington, DC.

Table 1: List of round vessel models

Bulge type	Bulge depth (in)	Fillet radius (in)	Bulge radii (in)		Bulge size (in)		aspect ratio
			Vertical	Horizontal	Length (circumferential)	Width (axial)	
spherical	2	20	100	100	92.5	43.6	2.12
spherical	2	40	100	100	93.5	47.2	1.98
spherical	2	80	100	100	94.8	53.5	1.77
spherical	1	40	100	100	68.4	33.4	2.05
spherical	3	40	100	100	110.8	57.7	1.92
spherical	4	40	100	100	124	66.5	1.86
spherical	4	40	75	75	80.3	60.1	1.34
spherical	4	40	50	50	58.1	53.1	1.09
spherical	4	40	25	25	42.6	44.9	0.95
spherical	2	40	75	75	58.6	42.7	1.37
spherical	2	40	50	50	42	37.7	1.11
spherical	2	40	25	25	30.8	32	0.96
ellipsoidal	2	40	50	75	105.5	37.7	2.80
axisymmetric	2	40	50	N/A	754	37.7	10.00

Table 2: List of oval vessel models

vessel ovality ratio	Bulge location	Bulge depth (in)	Fillet radius (in)	Bulge radii (in)		Bulge size (in)		aspect ratio
				Vertical	Horizontal	Length (circumferential)	Width (axial)	
	no bulge							
	long side	2	40	25	25	30.9	32	0.966
1.25	short side	2	40	25	25	30.8	32	0.963
	no bulge							
	long side	2	40	25	25	31.1	32	0.972
1.54	short side	2	40	25	25	31.3	32	0.978
	no bulge							
	long side	2	40	25	25	31.3	32	0.978
2	short side	2	40	25	25	34.3	32	1.072

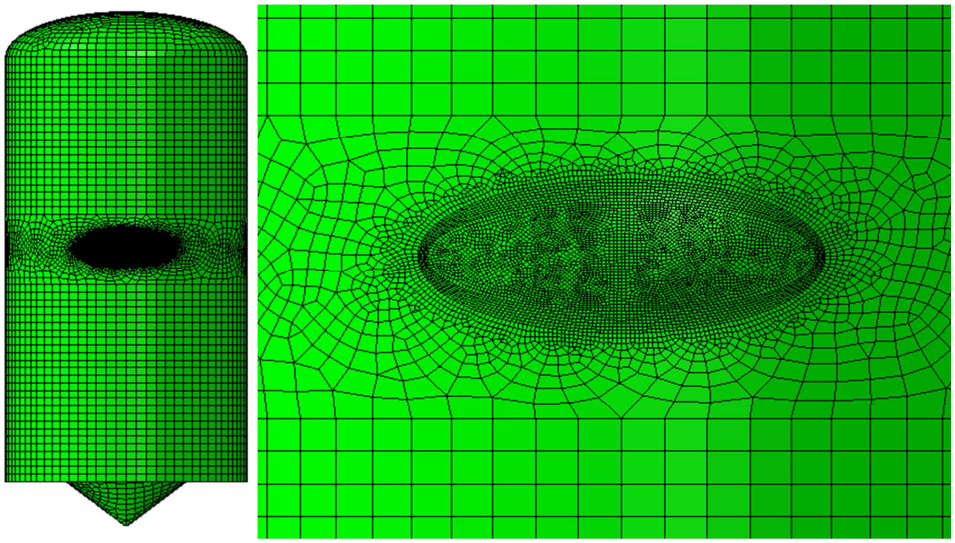

Figure 1: Typical mesh

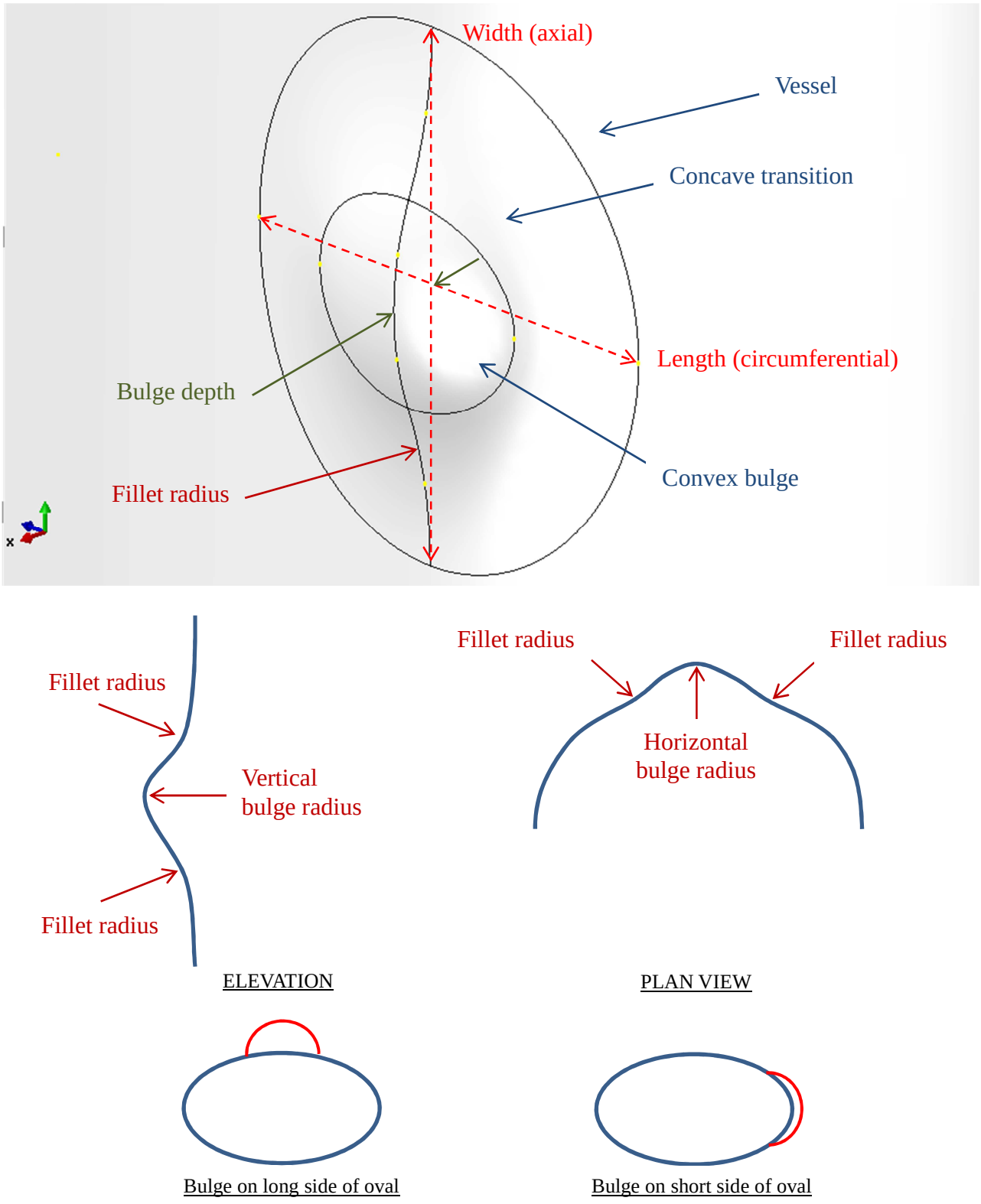

Figure 2: Schematic of bulge characteristics

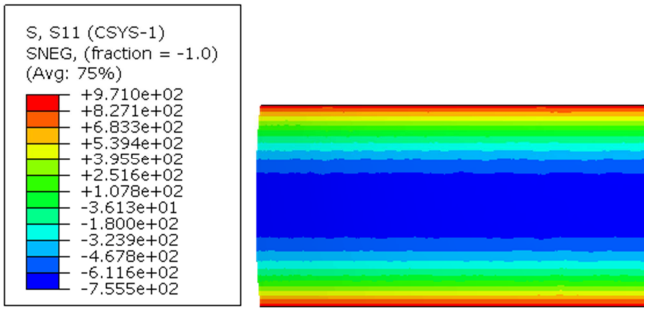

Figure 3: Axial stress on the inside of an example axisymmetric bulge (depth=2", Fillet=40", V-radius=50")

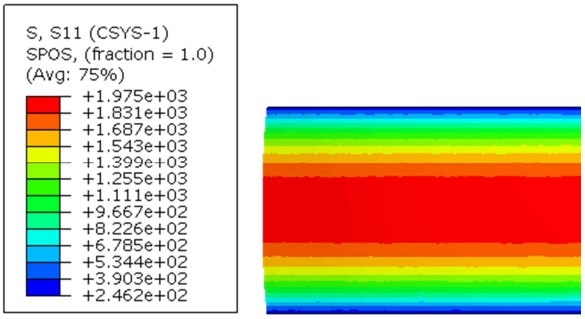

Figure 4: Axial stress on the outside of an example axisymmetric bulge (depth=2", Fillet=40", V-radius=50")

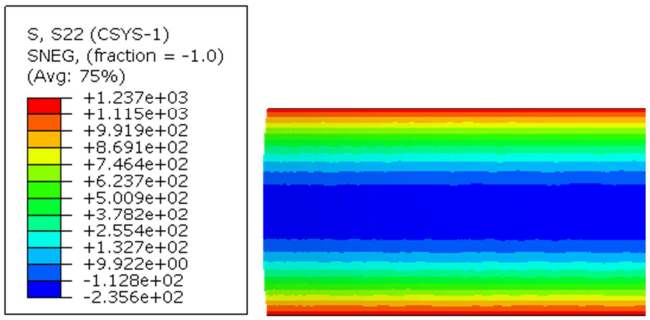

Figure 5: Hoop stress on the inside of an example axisymmetric bulge (depth=2", Fillet=40", V-radius=50")

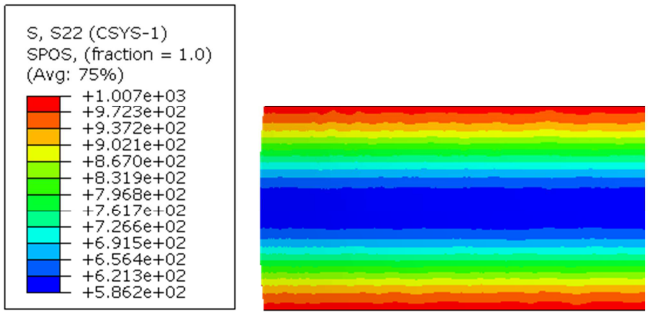

Figure 6: Hoop stress on the outside of an example axisymmetric bulge (depth=2", Fillet=40", V-radius=50")

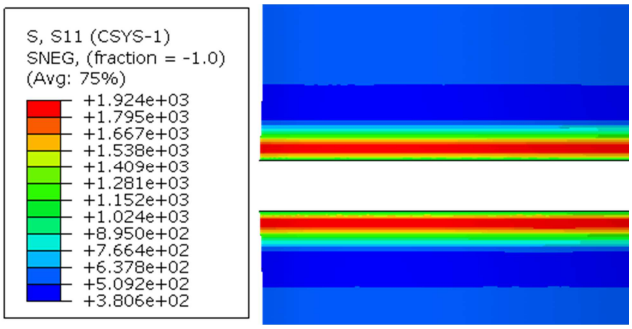

Figure 7: Axial stress on the vessel inside for an example axisymmetric bulge (depth=2", Fillet=40", V-radius=50")

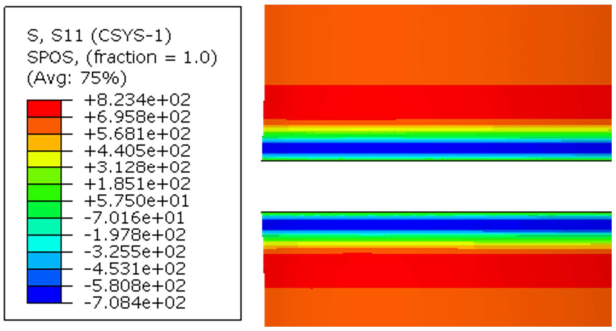

Figure 8: Axial stress on the vessel outside for an example axisymmetric bulge (depth=2", Fillet=40", V-radius=50")

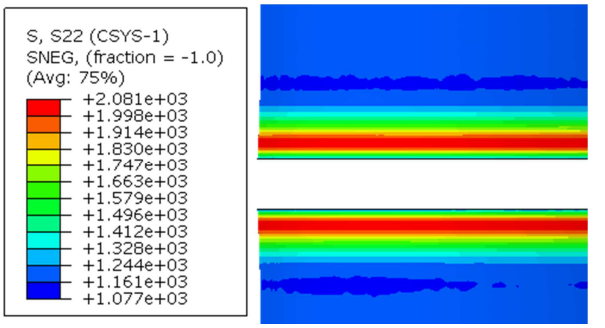

Figure 9: Hoop stress on the vessel inside for an example axisymmetric bulge (depth=2", Fillet=40", V-radius=50")

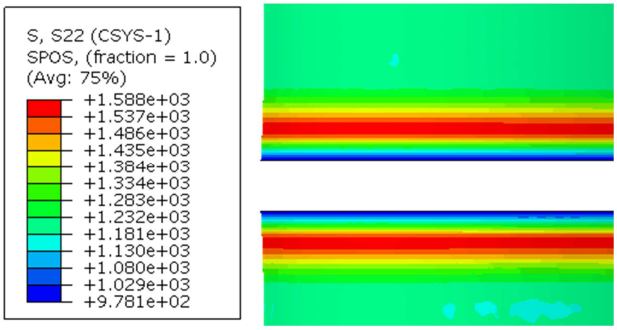

Figure 10: Hoop stress on the vessel outside for an example axisymmetric bulge (depth=2", Fillet=40", V-radius=50")

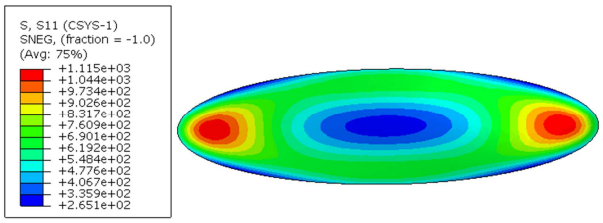

Figure 11: Axial stress on the inside of an example local bulge (depth=2”, Fillet=40”, V/H-radius=100”)

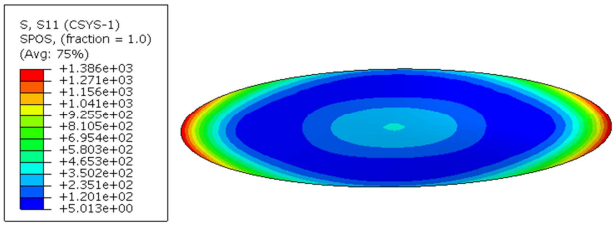

Figure 12: Axial stress on the outside of an example local bulge (depth=2”, Fillet=40”, V/H-radius=100”)

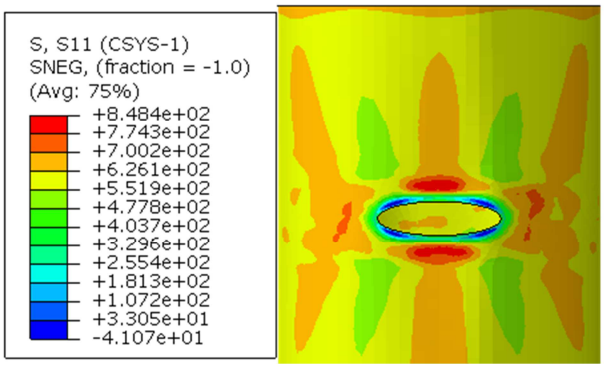

Figure 15: Axial stress on the vessel inside for an example local bulge (depth=2”, Fillet=40”, V/H-radius=100”)

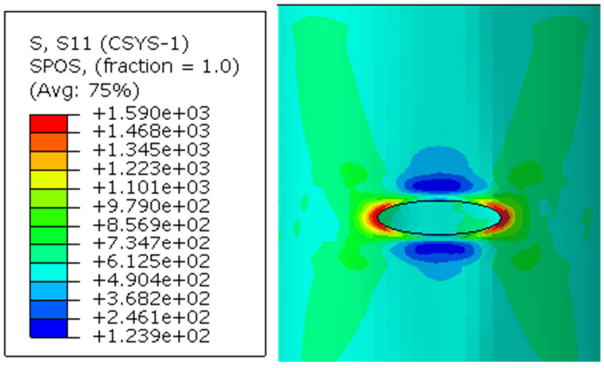

Figure 16: Axial stress on the vessel outside for an example local bulge (depth=2”, Fillet=40”, V/H-radius=100”)

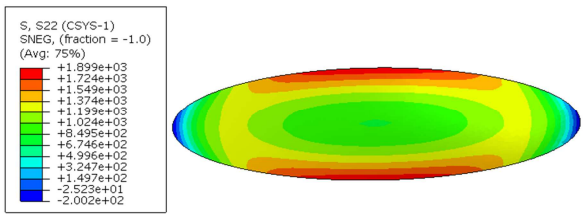

Figure 13: Hoop stress on the inside of an example local bulge (depth=2”, Fillet=40”, V/H-radius=100”)

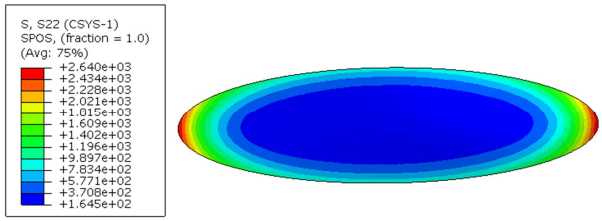

Figure 14: Hoop stress on the outside of an example local bulge (depth=2”, Fillet=40”, V/H-radius=100”)

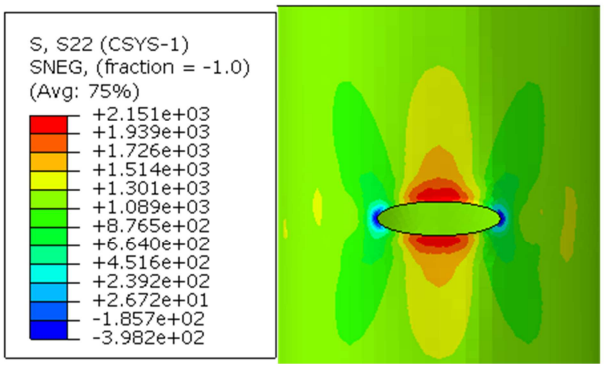

Figure 17: Hoop stress on the vessel inside for an example local bulge (depth=2”, Fillet=40”, V/H-radius=100”)

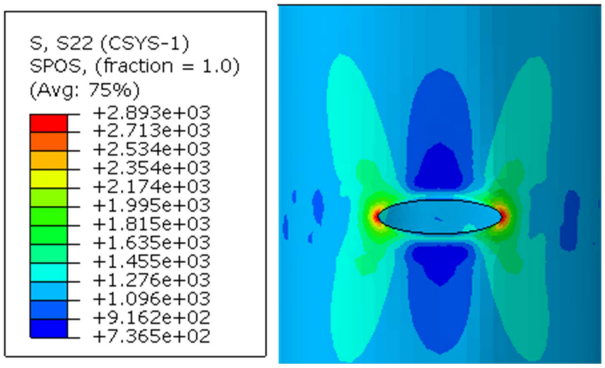

Figure 18: Hoop stress on the vessel outside for an example local bulge (depth=2”, Fillet=40”, V/H-radius=100”)

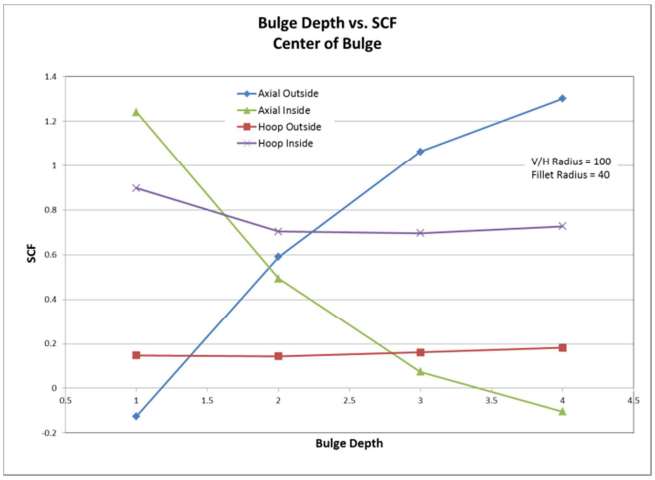

Figure 19: SCF at the center of the bulge vs. bulge depth

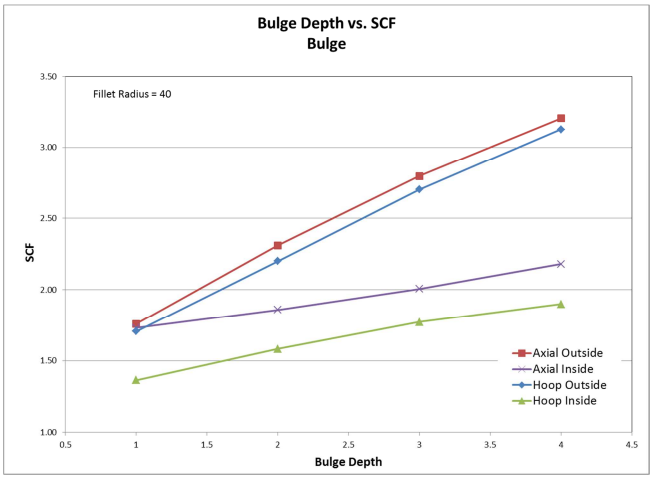

Figure 20: Maximum SCF in the bulge vs. bulge depth

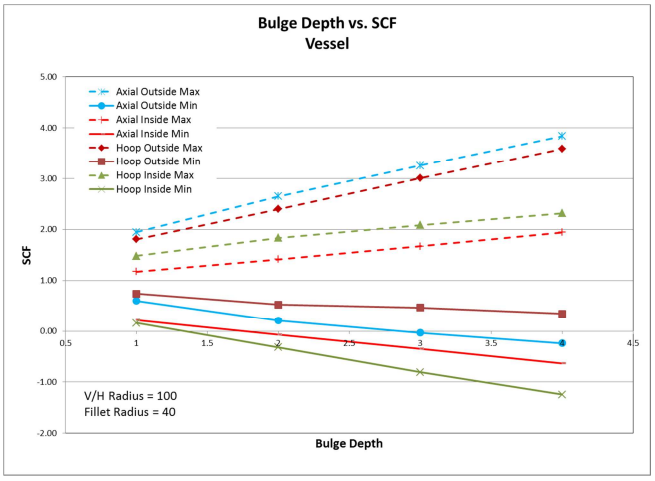

Figure 21: SCF in the vessel vs. bulge depth

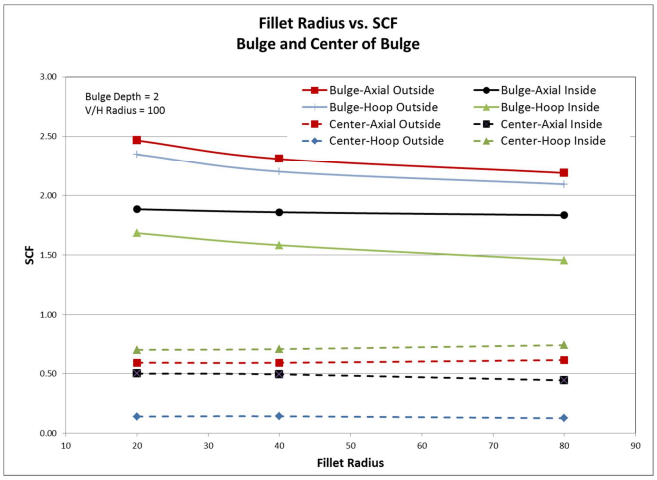

Figure 22: SCF in the bulge and center of bulge vs. fillet radius

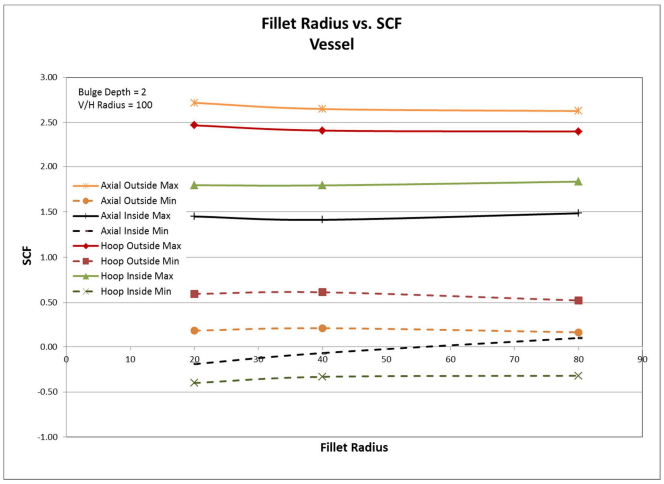

Figure 23: SCF in the vessel vs. fillet radius

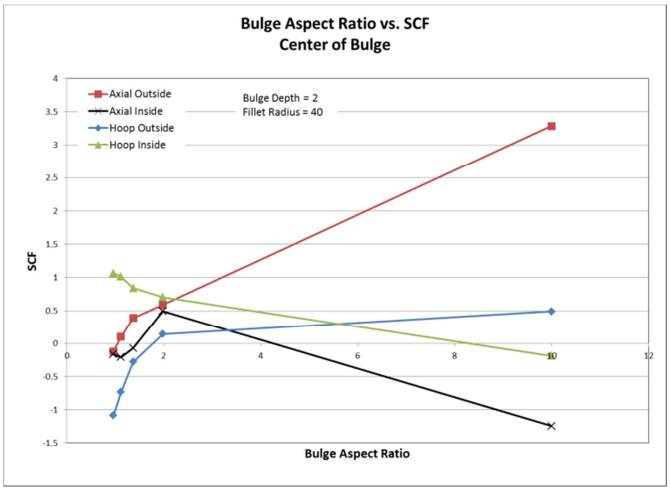

Figure 24: SCF at the center of a 2" deep bulge vs. aspect ratio

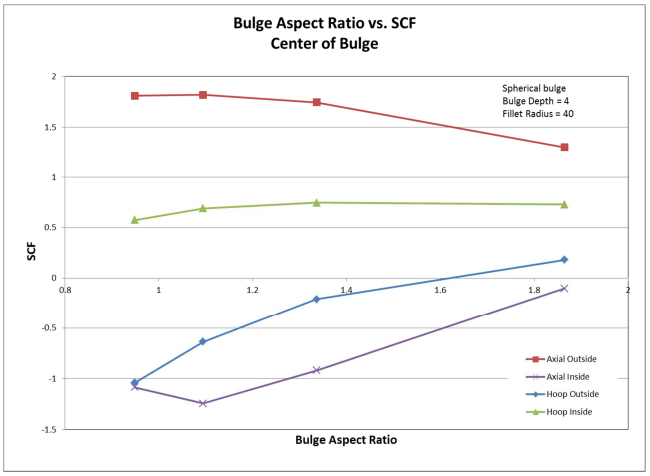

Figure 25: SCF at the center of a 4” deep bulge vs. aspect ratio

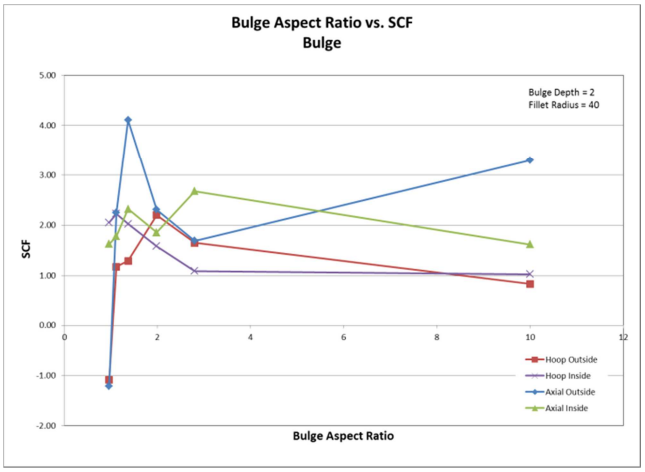

Figure 26: SCF in a 2” deep bulge vs. aspect ratio

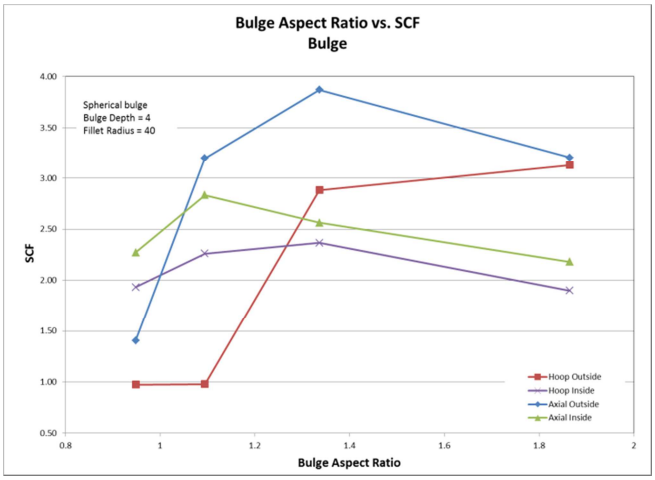

Figure 27: SCF in a 4” deep bulge vs. aspect ratio

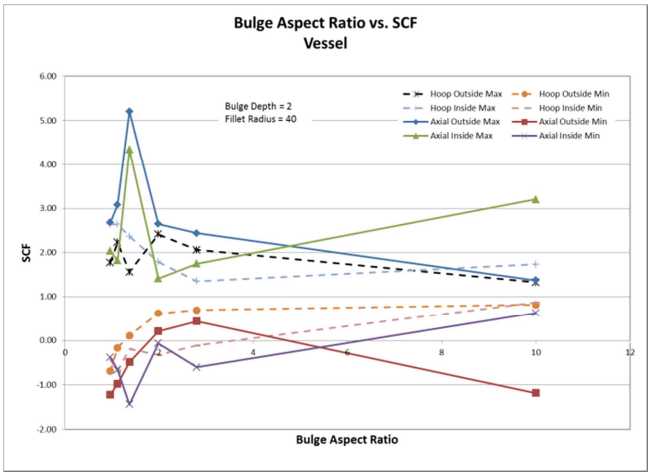

Figure 28: SCF in the vessel due to a 2” deep bulge vs. aspect ratio

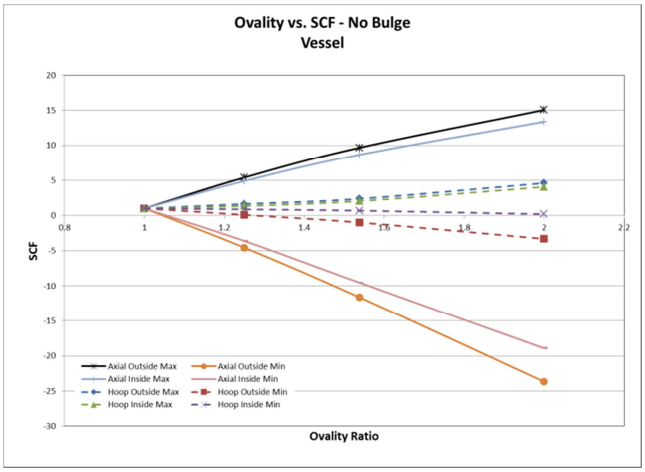

Figure 29: SCF in an oval vessel without a bulge

Figure 30: SCF in an oval vessel with a 2” bulge on the short side

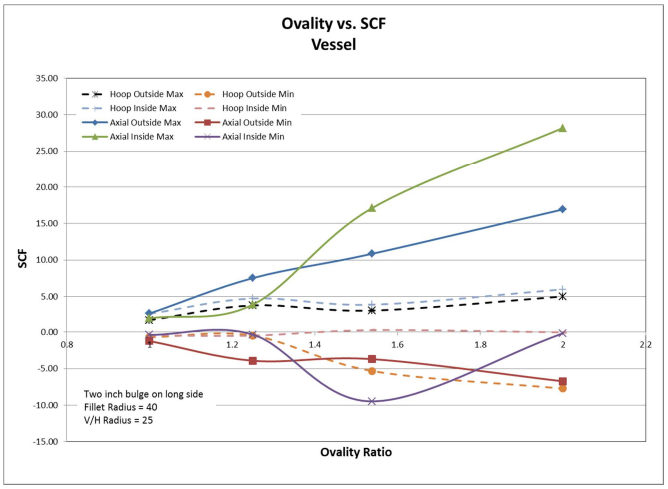

Figure 31: SCF in an oval vessel with a 2” bulge on the long side

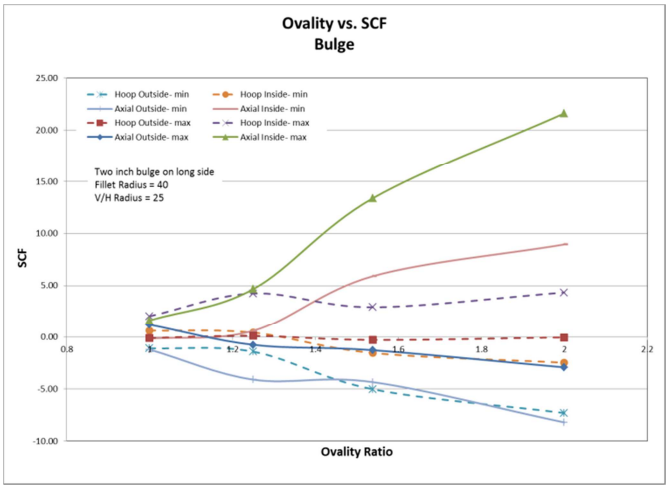

Figure 33: SCF in a 2” bulge on the long side an oval vessel

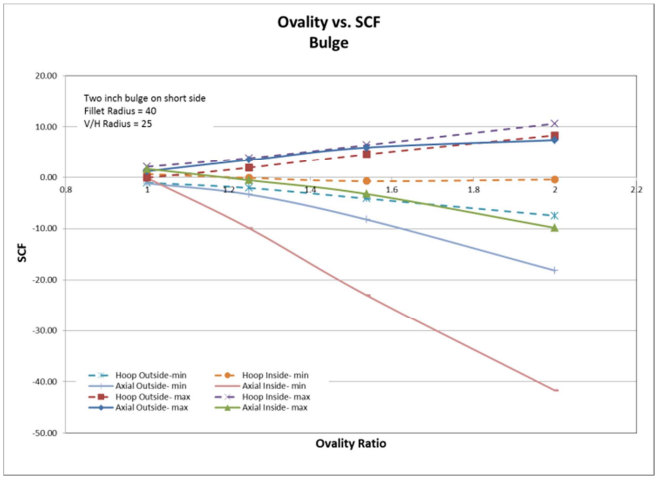

Figure 32: SCF in a 2” bulge on the short side an oval vessel

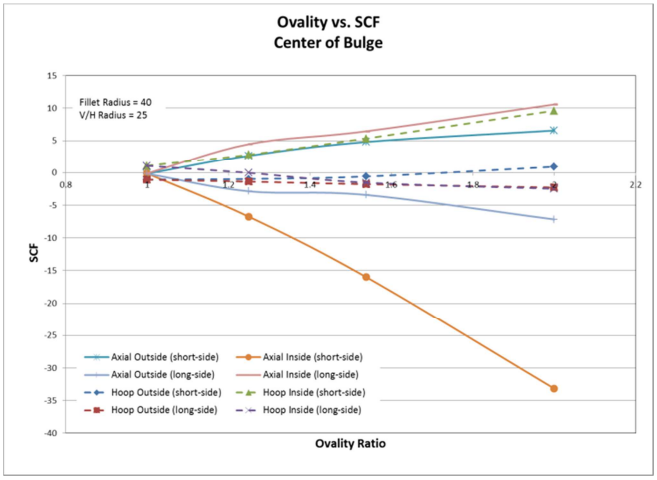

Figure 34: SCF at the center of a bulge on the long and short sides of an oval vessel